Improving Equipment Reliability utilizing Digital Image Correlation Photogrammetry

Dale "DJ" Winterhoff, Trilion Quality Systems

Dale Winterhoff, Flowserve

Abstract

A large refinery in Canada's tar sands, experienced 9 mechanical seal failures in 3 months on their critical service vacuum bottom pumps. The standard FEA analysis, was unable to conclusively resolve the observed failure modes. However, additional optical field measurements, using TRITOP Photogrammetry and ARAMIS Digital Image Correlation Photogrammetry, showed an angular displacement which, when calculated, presented significant nozzle loading in excess of 8x API loading statures in all axes. Using these optical measurement results as an input, an improved FEA model could correctly illustrate the failure modes. Recommendations to the plant included a redesign of the piping headers as well as modifications to the pump baseplates. A new cartridge seal was also recommended that was more tolerant of the displacements observed and resulting vibrations. Since the redesign and installations, the plant has yet to experience a unit failure. The identified issues would not have been possible without TRITOP and ARAMIS field optical measurements.

Introduction

A large refinery in North America was experiencing low mean time between failures (MTBF) on their critical service vacuum bottom pumps. Three single stage pumps running in parallel, each capable of 6000 gallons per minute, 700 feet of head and running at 3600 RPM. The pumps featured a between bearings design, with the impeller between the two sets of bearings, as well as a radially split casing. These pumps experienced 9 mechanical seal failures in 3 months. Due to American Petroleum Institute (API) regulations, the mechanical seals featured a double front to front style design, with a 53B flush plan to completely mitigate the possibility of service leakage to atmosphere. The outer seal was typically the first to fail and would leak at varying rates depending on the configuration of pumps currently in service. Picture 1 shows pumps A, B and C (from right to left), as well as discharge line (green, right of each pump) and suction line (blue, left of each pump).

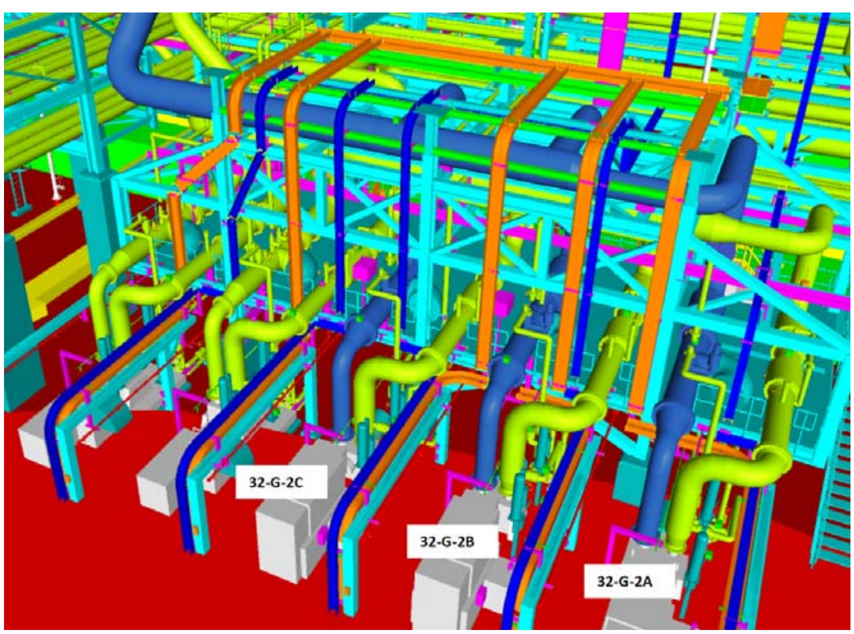

Figure 2 - Photo of refinery showing pumps of concern, and scale of the measurements.

These failures lead to a 38% reduction in production capacity. In an effort to meet the production demands, the pump in operation was set to operate to the right of its curve, near 120% of its best efficiency point (BEP), which lead to the development of a host of new problems. In addition, the wear ring clearances were opened to 0.050” to allow for the increased radial movement in an attempt to prevent the rapid seal failure during start-up. These measures resulted in reduced hydraulic performance as well as introduced recirculation issues which was verified by the presence of a dominant vane pass (5x run speed) during pretest vibration analysis and as seen in the dynamic pressure data.

A Finite Element Analysis model was created, utilizing current API regulations data, in an attempt to eliminate the pump as the failure mechanism. However, the model was unable to reconcile the table top model with the observed failures seen in the field. This allowed for the possibility of an unknown factor contributing to the failure mode observed.

Optical Measurements

In order to test the hypothesis that the poor piping design was the culprit, a large scale optical metrology solution was employed. Optical metrology systems, a 3D photogrammetry method, utilize an image series in conjunction with target and reference markers to discern micrometer level displacements, even when employed on the scale of the unit (180,000 cubic feet). TRITOP photogrammetry, a portable optical coordinate measuring machine (CMM), capable of quasi static 6 degree of freedom measurements, was used to validate the claims. TRITOP can also image and measure the entire volume of the pipes, pumps, motors and pads, referenced to the fixed building floor, columns and beams.

Due to known piping displacement concerns pump B was unable to run reliably and pump A was in operation during the start of the test. Therefore, the test cycle involved bringing Pump C up to temperature during which time data would be collected. The measurement included a baseline image series at ambient temperature, which all future measurements were to be compared against. Measurements were taken at 200°F, 400°F and hot standby (473°F), during the warmup phase of Pump C, as well as acquiring data at predetermined intervals during the cool down of Pump A (see test cycle table below). In order to obtain the data to prove the hypothesis, target markers were placed on critical components of the unit including different points along the suction and discharge lines, and headers, baseplates, motors, as well as the pumps and pedestals. Since the TRITOP measurement series is a quasi-static, time independent measurement, it was necessary to employ another form of optical metrology to ensure some unknown factor was not accounting for the failure mode observed.

Table 1. Test cycles.

Test Cycle	Pump A	Pump B	Pump C
1	Operational	Unbolted	Unbolted, off
2	Operational	Unbolted	Bolted off
3	Operational	Unbolted	Steam @ 200°F
4	Operational	Unbolted	Steam @ 400°F
5	Operational	Unbolted	Hot Standby
6	Hot Standby	Unbolted	Operational
7	Steam @ 200°F	Unbolted	Operational
8	Cold, unbolted	Unbolted	Operational
9	Hot Standby	Unbolted	Operational
10	Hot Standby	Bolted with Blinds	Operational
11	Operational	Bolted with Blinds	Hot Standby

The high-speed ARAMIS metrology tool (Digital Image Correlation Photogrammetry) was employed to obtain both full field 3-D displacements and vibrational data on key components of the bad actor pumps. The ARAMIS tool utilizes target markers similar to those used in TRITOP, but allows for fast stereo acquisition measurements to discern relative movements between components in real-time. ARAMIS target dots and patterning were affixed to the pump casing, bearing housings, seal glands, coupling and shaft in an effort to obtain both vibration signatures as well as to validate the hot alignment procedures. ARAMIS measurements were acquired at the same points of the test cycle to assist in determining the failure modes. Below are target dots placed on key components for 6 DOF measurements.

Figure 3 - Target dots seen on key equipment and piping. Picture on left shows the Suction/Discharge lines, where the largest piping displacements were seen. Picture on right, shows Pump C motor and baseplate with photogrammetry targets.

Due to the interconnectivity of the shared suction and discharge headers, changes to any one pump in the system affected change on another. During the warmup phase of the test, forces due to thermal expansion would allow for deformation of not only the piping structure but the pump casings as well. As the casings come to temperature, they will become mechanically loaded according to which way the piping is pulling. According to the vector displacement of that expansion, this will result in the casing shifting and departing a force onto the baseplate. Since alignment of the shaft to the motor is critical for ensuring proper reliability of the system, this expansion needs to be either removed or accounted for in the hot alignment process. When the pump finally reaches its operating temperature, it is started and given time to reach its operating speed whereby the discharge valve is opened allowing the service to flow throughout the entire system. This opening of the discharge valve introduces pressure forces which can introduce sources of vibration that can be damaging to the pump. Once the pump is in operation, all the aforementioned factors will become sources for vibration. For instance, misalignment of the shaft will introduce a damaging frequency that can be seen in the FFT data collected, as would vane pass pressure pulsations coming from the on-line pump or upstream from the sister pump.

Since all of the aforementioned forces were to be measured to paint a picture of the failure mode, single point accelerometers, dynamic pressure gauges, thermal imagers and a wireless shaft strain gauge system were also utilized. The accelerometers allowed for operational deflection shape analysis of the pumps and motors while the dynamic pressure gauges ensured that a larger system issue upstream wasn’t at fault. The thermal imager was employed to observe temperature profiles during the test cycle, and a wireless strain gauge was utilized on Pump C to identify shaft bending and strain across the coupling during startup.

To kick off the test, a baseline TRITOP photogrammetry image series was acquired to discern the zero-point, or 3D reference position, for all components comprising the test. The baseline condition featured Pump A in high temperature operation, with both the suction and discharge lines at service temperature(473F), Pump B unbolted from suction and discharge lines, and Pump C bolted, but isolated and drained. Vibration data was collected on Pump A to perform a baseline operational deflection shapes (ODS), while the dynamic pressure sensors registered the signatures of pumps. ARAMIS was used to collect vibration data on Pump A to corroborate with the ODS results.

All of the aforementioned measurements and measurement techniques were repeated throughout all points in the test cycle over a period of 3 days, to fully illustrate all the factors at play. The high-speed ARAMIS shaft analysis was performed at startup of Pump C, to acquire vibrational data, to observe the effects of the piping header displacement on the seal during startup and at predetermined intervals thereafter.

At the conclusion of the test, it was evident that the casing was in fact distorting, due solely to the large displacements of the suction and discharge piping. TRITOP had registered suction and discharge displacements on the scale of an inch, which were leading to the increased nozzle loads and excessive stress on the pump casing. To substantiate this conclusion, the time lapse ARAMIS measurements taken on the pump casing corroborated the vector displacements seen in the TRITOP results throughout every phase of the test cycle. A novel feature of the TRITOP tool is the ability to perform rigid body motion corrections (RBMC) to use one component as a static reference to compare all motion against. This feature was utilized to identify 0.06” displacements between the motor and the baseplate, as the pump was brought to temperature. This highlighted the need for increased attention during the hot alignment procedures. The TRITOP data also showed a torsional displacement of 0.110” towards the discharge, as looking from the drive end, throughout the test. This led to the conclusion that the baseplate was deflecting and after further investigation it was determined that it was installed with large voids allowing it to move. Displacements as large as 2 inches were seen at the piping headers which allowed for the torqueing motion seen at the pump nozzles. (see figures below)

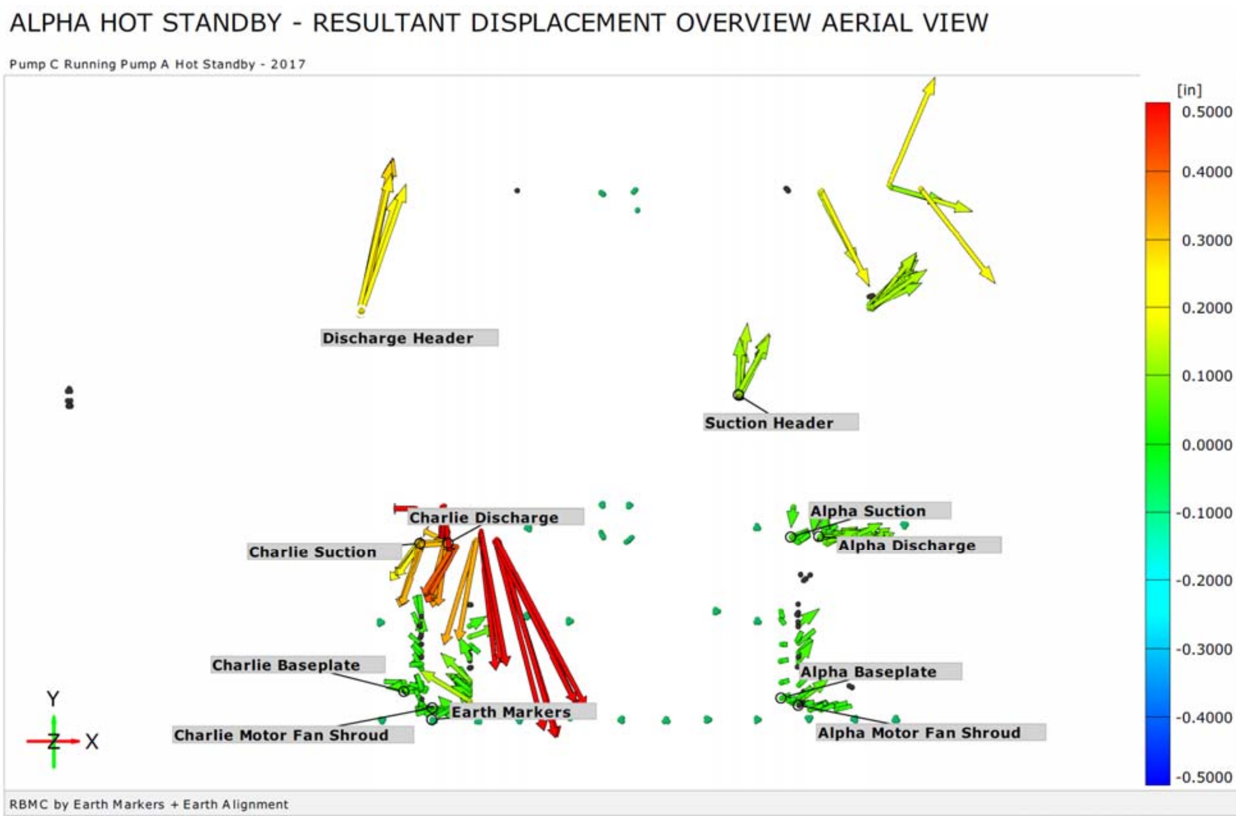

Figure 4 - TRITOP 3D coordinate map showing how bringing one pump to temperature affects another.

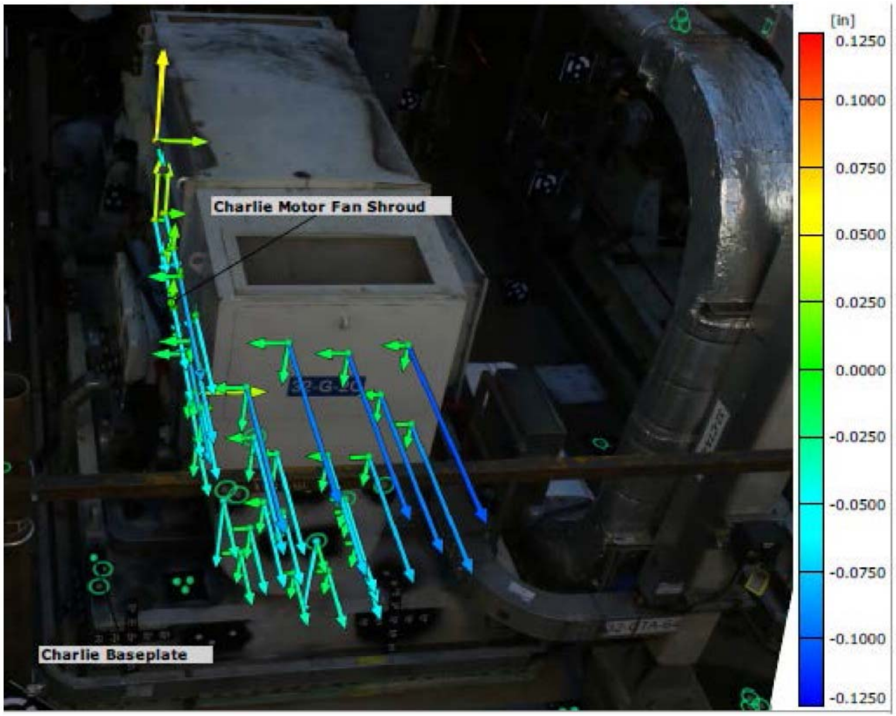

Figure 5 - Pump C motor showing torsional motion while on baseplate. This confirmed suspicion of . Improper baseplate grouting

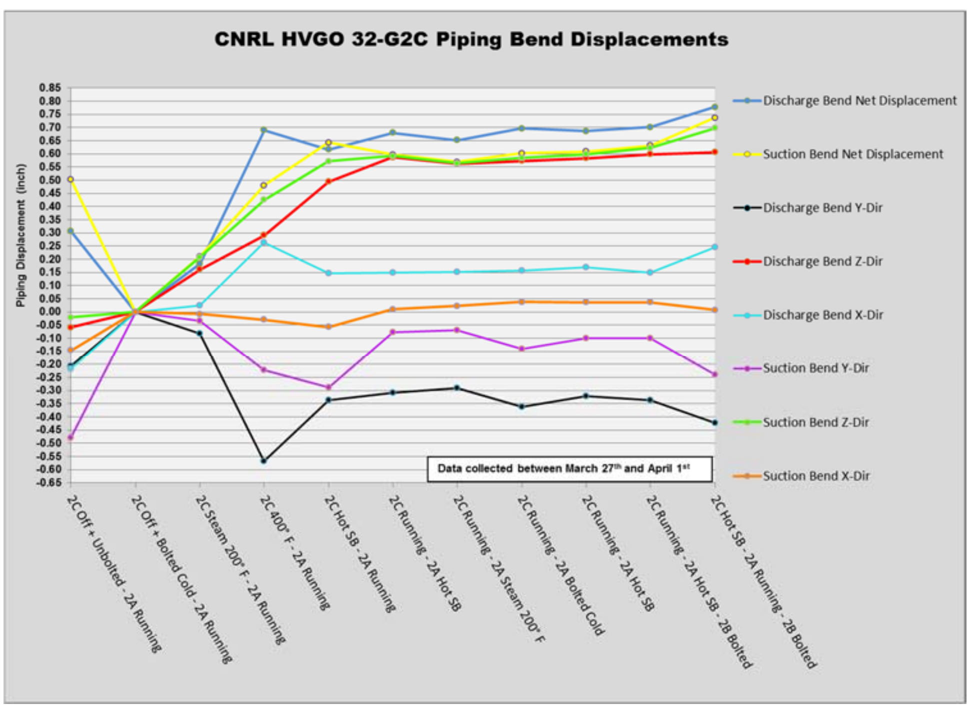

Figure 6 - Displacements of Pump C suction / discharge line throughout the test cycle. Need to REMOVE the plant name in the header CNRL – I have the original if you need it

The FFT vibration data collected on Pump A, showed consistent frequency peaks at 1x, 2x, 5x and 10x to run speed in every axis. There was a decrease in amplitude as Pump C was brought to temperature. The high-speed ARAMIS data corroborated these findings. ARAMIS also identified lower frequency issues caused by structural defects in the baseplate. The TRITOP data also showed excessive deformation due to the structural defects in the baseplate. A seal barrier fluid leak on Pump A, was observed at the beginning of the warmup phase of Pump C. This gradually decreased as the test cycle progressed, and eventually ceased when Pump C reached its operating temperature. It is noteworthy to explain that when the seal finally stopped leaking, the amplitudes of the 1x and 2x frequencies on Pump A also decreased substantially. This revelation confirmed that the piping displacements were inhibiting reliable operation of the pumps.

The plant had initially expressed concern with the current hot alignment procedures due to the fact that multiple seals had failed during startup. The ARAMIS shaft analysis performed substantiated their need for concern by identifying a 0.040” runout radially, while identifying a 0.160” axial thrusting on the outboard motor side, which translated to a 0.045” axial thrusting on the inboard pump side. This is alarming when considering the effect this axial thrusting has on the double mechanical seal on the pump. The shaft analysis also identified a 1-degree angular misalignment during startup which reduced to 0.6 degrees as the test progressed. The ARAMIS analysis also validated the findings of both the ODS and shaft strain gauges when identifying an elliptical orbit due to the misalignment.

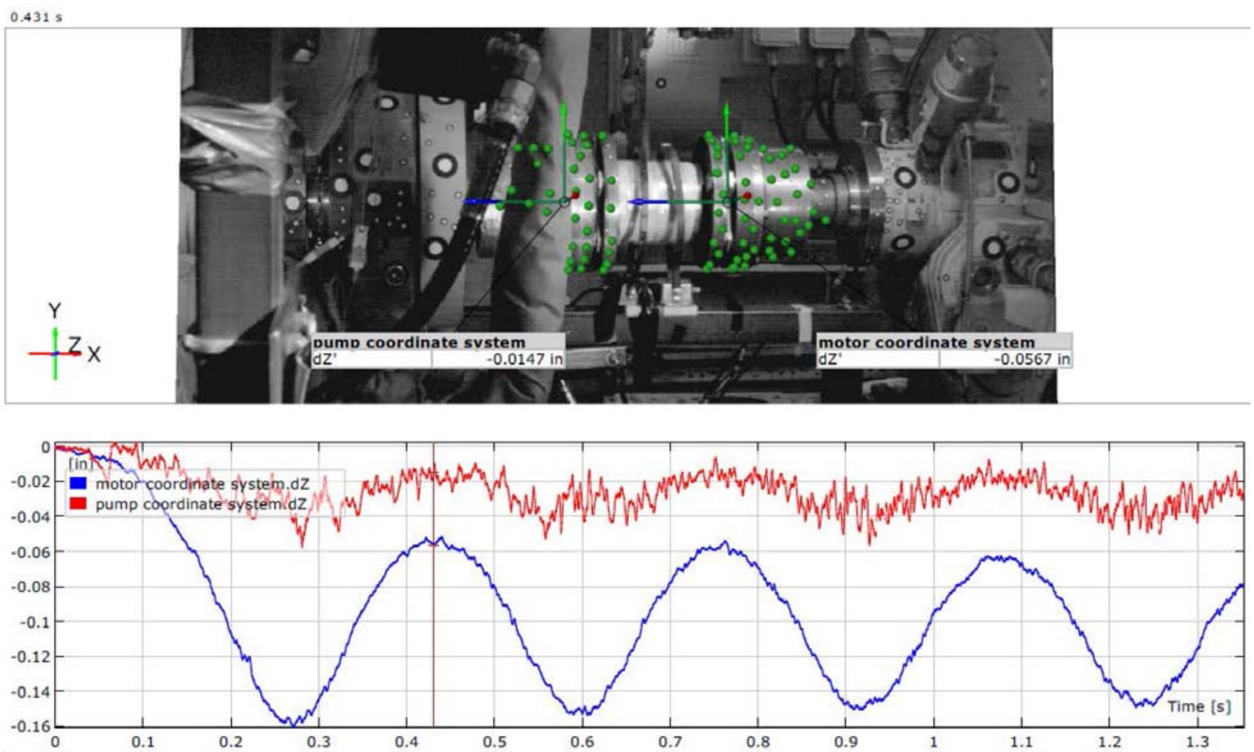

Figure 7. High Speed ARAMIS shaft analysis showing shaft axial thrusting during startup. Thrusting on outboard motor side is transferred through coupling translating to a 0.40” impacting on seal faces and bearings.

A post-test FEA was performed using the optical TRITOP and ARAMIS data as the input. As mentioned previously the standard FEA was unable to account for the observed failures. It should be noted that a standard FEA applies force to the centerline of the nozzle. Conclusions from this type of analysis can be misleading as real world forces occur in multiple directions. The optically acquired TRITOP and ARAMIS photogrammetry data showed an angular displacement, which when calculated showed nozzle loads in excess of 8Xx rated API loading statures in all axes. This fact highlights the ability of TRITOP and ARAMIS photogrammetry to complement current FEA practices to create smarter models to identify failure modes.

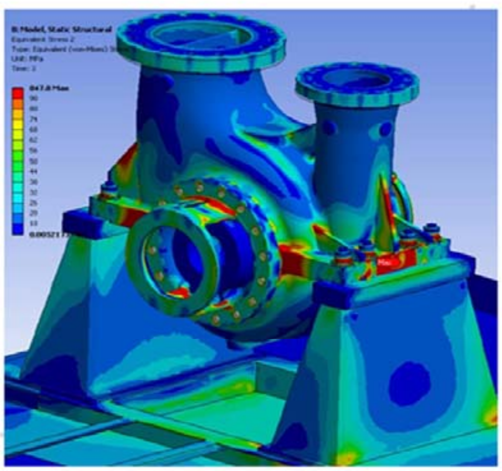

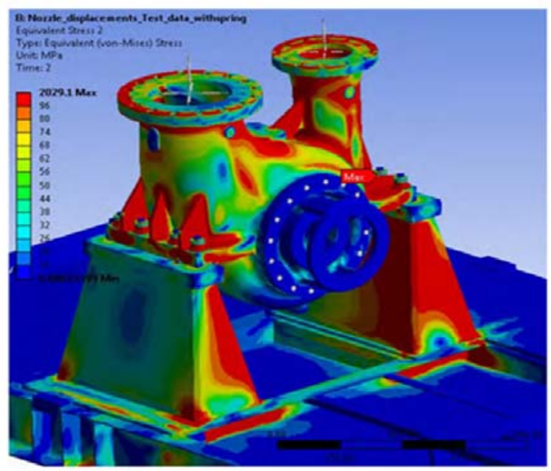

FEM using traditional inputs on left showing 8x API regulations for nozzle loading versus the optically acquired TRITOP / ARAMIS inputs on right showing nozzle loading in excess of 16x API regulations

The test results elucidated to the fact that roughly 197kW of excess power were consumed due to the efficiency losses. This equated to $207,000 a year on energy losses alone, not to mention the missed opportunities from decreased production stemming from the seal failures. Recommendations to the plant included a redesign of the piping headers as well as modifications to the pump baseplates. A new cartridge seal was also recommended allowing for increased vibrations. Since the redesign and installations, the plant has yet to experience a unit failure. It is important to note that many of the identified issues would not have been possible without the use of TRITOP and ARAMIS. Without he insights gained from deploying this technology, management would have continued with costly short term tactical repairs and would still be experiencing the failures.

Acknowledgements

This work was performed with ARAMIS and TRITOP photogrammetry equipment and engineering support from Trilion Quality Systems, King of Prussia, PA (www.trilion.com). This work was performed under a contract and with the direct engineering support of Flowserve Corporation, Bethlehem, PA (www.flowserve.com).

References

1. Alpers, B., Bergmann, D., Galanulis, K., Winter, D.: Advanced deformation measurement in sheet metal forming, Proceedings of the 6th ICTP, September 1999
2. Tyson, J., Schmidt, T., Galanulis, K. Advanced Photogrammetry for Robust Deformation and Strain Measurement, Proceedings of the 2002 SEM Annual Conference & Exhibition of Experimental and Applied Mechanics, June 2002
3. Hoffmann, H., Vogl, C., Determination of True Stress-Strain-Curves and Normal Anisotropy in Tensile Tests with Optical Strain Measurement STC F, 52/1/2003, p.217 CIRP Annals – 2003
4. Schmidt, T., Tyson, J. & Galanulis, K., “Full-Field Dynamic Displacement and Strain Measurement Using Advanced 3D Image Correlation Photogrammetry,” Experimental Techniques, 27(4), 22-26 (2003).
5. Tyson, J, Schmidt, T, Coe, D, Galanulis, K., “3D Image Correlation for Dynamic and Extreme Environment Materials Measurements Holistic Structure Measurements from the Laboratory to the Field,” *SEM 2005 Conference Proceedings*, Portland OR, June, 2005.
6. Paulsen, U., Erne, O., Schmidt, T., “Wind Turbine Operational and Emergency Stop Measurements Using Point Tracking Videogrammetry,” Proceedings of IMAC-XXVIII, Jacksonville, Florida February 2, 2010.
7. Niezrecki, C. and Avitable, P., Digital Image Correlation Applied to Structural Dynamics, Proceedings of IMAC-XXVII, Orlando, FL, February 2009.
8. Pickrel, C.R., A Possible Hybrid Approach for Modal Testing of Aircraft, Proceedings of IMAC-XXVII, Orlando, FL, February 2009.
9. ARAMIS, v. 6.3.1 User’s Manual, Revision H, GOM mbH, Braunschweig, Germany (2014)
10. Tyson, J., Psilopoulos, J., Schwartz, E., Galanulis, K. Advanced Material Properties Measurements with Optical Metrology, Proceedings SAE Annual Conference 11M-0343, April 2011.
11. Tyson, J., Optical 3D Deformation and Strain Measurement, *Nondestructive Testing Handbook*, Third Edition: Vol. 10, *Nondestructive Testing Overview,* American Society of Nondestructive Testing (2012): Chapter 15, Section 2, pg. 507-511.

12. Knoerr, L, Sever, N., Faath, T., "Cyclic Tension Compression Testing of AHSS Flat Specimens with Digital Image Correlation System", Proceedings NUMISHEET Annual Conference 2014.

13. Tyson, J., Schmidt, T., Psilopoulos, J., Optical Metrology the Key to Lean Manufacturing, SAMPE Baltimore Conference, Composite Applications in the Automotive Industry, A-7545, April 2015.

14. Tyson, J., Psilopoulos, J., Factory of the Future, Design, Analysis and Verification, CAMX 2017, TP17-0141, Orlando, FL, December 2017.